© 1997 The Chemical Society of Japan Bull. Chem. Soc. Jpn., 70, 1109—1114 (1997)

Evidence for Spiro-Conjugation in Perpendicularly-Linked Pentamethinestreptocyanine Dimers

Takashi Katoh, Keizo Ogawa, Yoshio Inagaki, and Renji Okazaki*,†

Ashigara Research Laboratories, Fuji Photo Film Co., Ltd., 210 Nakanuma, Minami-ashigara, Kanagawa 250-01

†Department of Chemistry, Graduate School of Science, The University of Tokyo, 7-3-1 Hongo, Bunkyo-ku, Tokyo 113

(Received October 11, 1996)

Perpendicularly-linked pentamethinestreptocyanine dimers (**1**) in which the two cyanine moieties are linked at the center carbon atoms of the methine chains were prepared. The absorption spectra of **1** in solution showed two peaks at 446 and 406 nm, which are attributed to the splitting of the HOMO levels through spiro-conjugation between the two cyanine moieties, as calculated from the INDO/S-CI method. The reduction potential of **1** positively shifted with respect to that of the corresponding monomer (**2**). The oxidation polarogram of **1** showed two waves, with the first potential negatively shifting compared to that of **2**.

Many cyanine dyes form aggregates in aqueous solution, especially in silver halide photographic emulsion.1) Large spectral shifts observed on aggregation are attributed to exciton coupling, i. e., coupling of transition moments of the constituent dye molecules.2)

Heptamethinestreptocyanine dimers in which two cyanine moieties are covalently connected to form a V-shaped configuration at an angle of ca. 70 ° showed a splitting of an absorption band.3) The spectral features are explained in terms of exciton coupling, in which the excitonic state of a dye aggregate splits into two levels through interaction of transition dipoles (Fig. 1). However, the exciton model is probably an excessive simplification, because it is valid only when the interaction between orbitals of constituent molecules is negligible.4)

Kazmaier and Hoffmann reported that the nodal pattern of frontier orbitals of the constituent molecules reflected on the band width of π -stacked perylene molecules with a 3.5 Å of interplaner contact.5) It seems to be a reasonable postulate that intermolecular interaction of orbitals cannot be neglected also for aggregates of cyanine dyes, in which dye molecules are usually stacked with interplaner contact of ca. 3.5 Å.6)

An exciton model teaches us that a coupling of transition moments that lie perpendicularly to each other will not be observed. However, we found that the perpendicularly-linked pentamethinestreptocyanine dimers, prepared during the course of our study on cyanine dye aggregates, showed a distinct band splitting. The fact is worth investigating because it suggests that an interaction that has not been considered in the exciton model is operative. In this paper we account for this unusual band splitting in terms of spiro-conjugation over the perpendicularly arranged polymethine chains.

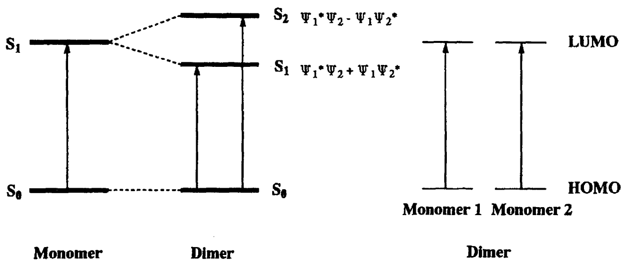

Fig. 1. Molecular exciton model. Two excited states of a dimer due to exciton coupling.

Results and Discussion

Synthesis. Perpendicularly-linked streptocyanine dimers (**1a** and **1b**) were prepared from a 4,4′-bipyridinium salt and aqueous dimethylamine in moderate yields (Scheme 1).

Structure. The ^{1}H NMR spectra of **1** in CD_3OD at 298 K consist of two doublets (*methine* protons, $J = 12$ Hz for **1a** and $J = 13$ Hz for **1b**) and two singlets (N-CH_3 protons), indicating all-*trans* conformations of the methine chains.

The molecular structure inferred from the NMR data was confirmed by single crystal X-ray crystallographic analysis for **1b** (Fig. 2), which revealed that **1b** is an all-*trans* conformer and that the two cyanine moieties are arranged perpendicularly to each other. The bond linking the two cyanine moieties is essentially a single bond, because the bond length between the two *meso*-carbon atoms of the methine chains is 1.503(7) Å, a typical single bond length between two sp^2 carbon atoms.

The molecular packing in the single crystal of **1b** (Fig. 3) indicates that the cyanine moieties make a brickwork-like stack with a separation of about 3.4 Å.

Absorption Spectra in Solution. The absorption spectra of **1a** and **1b** in methanol at 298 K are essentially the same, showing the two absorption bands at 446 and 406 nm

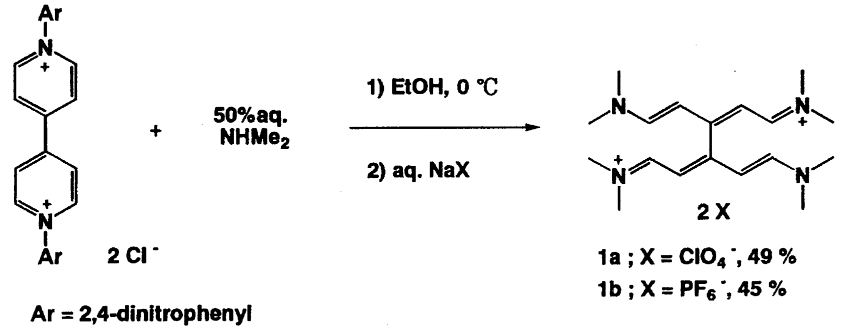

Scheme 1.

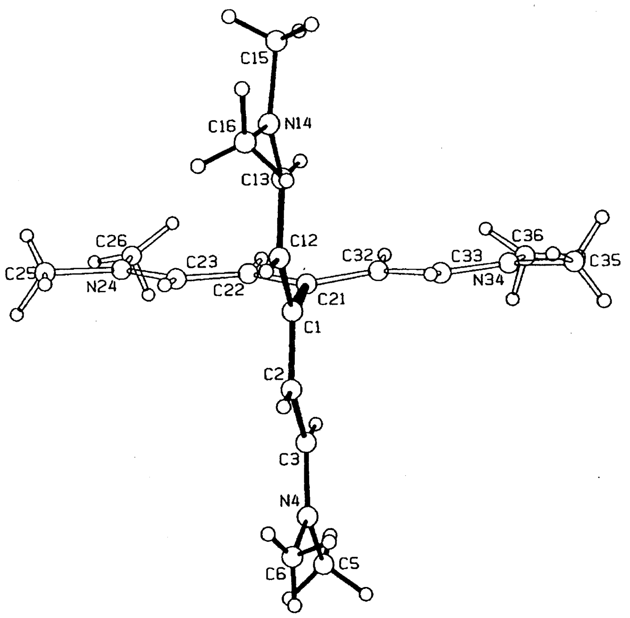

Fig. 2. The molecular structure of a streptocyanine dimer **1b**.

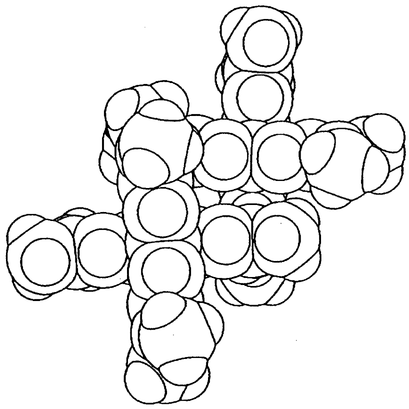

Fig. 3. The molecularl packing in a single crystal of a streptocyanine dimer **1b**.

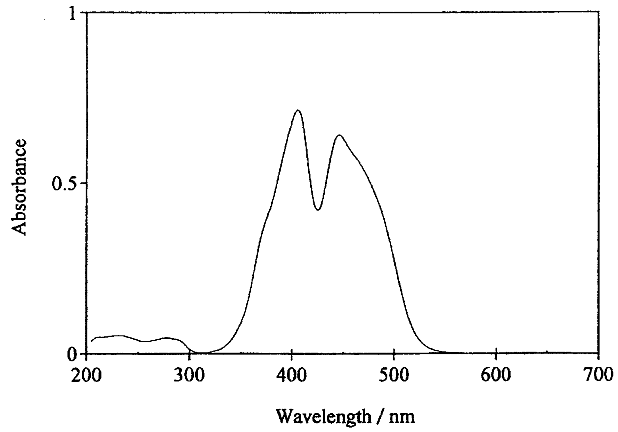

Fig. 4. An absorption spectrum of a streptocyanine dimer **1a** in methanol at 298 K (1.0×10^{-5} mol dm^{-3}).

(Fig. 4). The corresponding monomer, (5-dimethylamino-2,4-pentadienylidene)dimethylammonium perchlorate (**2a**) showed only one peak at 412 nm in methanol. The band splitting of **1** is not caused by intermolecular aggregation because the shape of the band is independent of solvents (methanol, water, *N*,*N*-dimethylformamide, acetone, and dichloromethane), concentration (1×10^{-5}—1×10^{-4} mol dm^{-3}), and temperature (200—333 K).

The following three cyanine dimers (Chart 1) have been reported to be linked between the carbon atoms of the methine chains.[7] Streptocyanine dimers (**3a** and **3b**) showed only one absorption band in methanol at 413 and 316 nm, respectively, and a cyanine dimer **3c** showed broad bands with two maxima at 545 and 520 nm in acetonitrile. However, the molecular structures of these dimers and the interactions between the two cyanine moieties remain unclear.

Molecular Orbital Calculations. The molecular structure for **1**, omitting counter anions was optimized with a PM3 method.[8] Calculations indicate that the orbital energy levels of **1** are lower than those of the corresponding monomer **2** and that the highest occupied molecular orbital (HOMO) levels of **1** are no longer degenerate (Fig. 5).

The magnitudes of orbital coefficients for **1** are shown in Fig. 6, which indicates that the coefficients of the two lowest unoccupied molecular orbitals (LUMOs) are localized on each cyanine moiety. On the other hand, the coefficients of HOMOs are delocalized on the whole of the two cyanine moieties and the splitting of HOMO levels is caused by a spiro-conjugation-like overlap of the two HOMOs of the cyanine moieties; the HOMO and next HOMO of the dimer correspond to out-of- and in-phase mode overlap, respectively. This phase relation is reminiscent of a spiro-conjugation for spiro-polyene compounds.[9]

The electronic absorption bands of **1** calculated with the INDO/S-CI method[10] using the optimized structure obtained

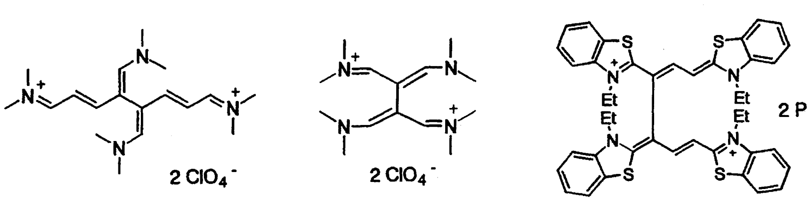

3a[7a)] **3b**[7b)] **3c**[7c)]

Chart 1.

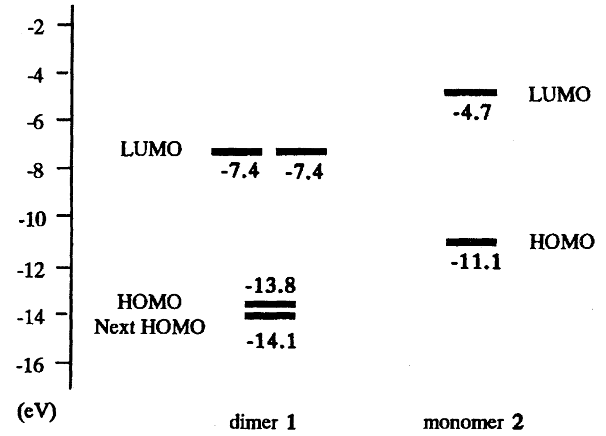

Fig. 5. Orbital energy levels for a streptocyanine dimer **1** and a monomer **2** calculated with the PM3 method.

with the MM2 method[11)] reproduced the splitting of the main absorption band (Table 1). The absorption at 433 nm is mainly due to the transitions from the HOMO to the LUMOs, and the absorption at 377 nm is mainly based upon the transitions from the next HOMO to the LUMOs. The splitting of the absorption band of **1** is caused by the splitting of the HOMO levels through spiro-conjugation (Fig. 7).

The strength ratio, 1.0 : 0.9, of the observed two bands around 406 nm and 445 nm of **1** in methanol was significantly different from the calculated ratio of the oscillator strengths, 1.0 : 0.45. In order to clarify the reason for the observed strength ratio and the contribution of the interactions between transition dipoles, the influence of molecular structures on the strength ratio of the two peaks was examined. The absorption bands of **1** in which the angle (θ) between the two cyanine moieties is fixed to be 80°, 70°, or 45° were calculated with the INDO/S-CI method.[10)] The results indicated that the oscillator strength of the shorter wavelength band increased with decreasing the angle (θ) (Table 2), suggesting that the difference between the observed and the calculated strength ratio does not originate from the interactions between transition dipoles.

In order to investigate the influence of configurations of methine chains of **1**, the oscillator strengths of mono-*cis* and di-*cis* conformers of **1** were calculated. The molecular

Table 1. Absorption Spectra of the Streptocyanine Dimer **1** Calculated with the INDO/S-CI Method[a)]

λ_{max}/nm	f[b)]	Transition character
433	0.45	0.98 (HOMO→LUMO)
433	0.45	0.98 (HOMO→LUMO)
378	1.00	0.98 (HOMO-1→LUMO)
377	1.01	0.98 (HOMO-1→LUMO)

a) The MM2 optimized structure was used. Counter anions were omitted. b) Oscillator strengths.

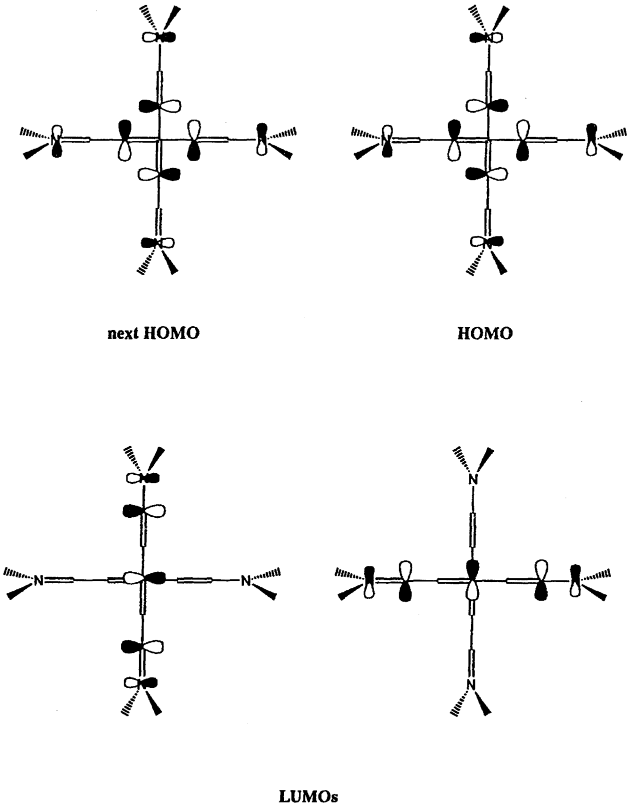

Fig. 6. Coefficients of the next HOMO, HOMO, and LUMOs of a streptocyanine dimer **1** calculated with the PM3 method.

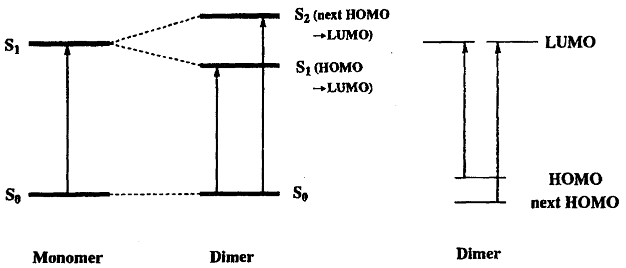

Fig. 7. Spiro-conjugation model. Two excited states of a dimer due to a splitting of HOMO levels.

Table 2. Dependence of Absorption Spectra of **1** on Angle (θ) between the Two Cyanine Moieties Calculated with the INDO/S-CI Method

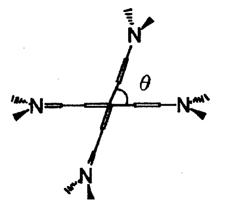

θ/degree	λ_{max}/nm ($f^{a)}$)
80	443 (0.43), 434 (0.50), 384 (0.72), 377 (1.17)
70	463 (0.34), 438 (0.45), 388 (0.55), 377 (1.46)
45	742 (0.03), 468 (0.01), 394 (1.85), 375 (0.16)

a) Oscillator strengths.

structures were optimized with the MM2 method without the counter anions. The calculated strength ratios of the two bands with the INDO/S-CI method were ca. 1 : 1.1 and 1 : 1.4 for the mono-*cis* and the di-*cis* conformers, respectively (Table 3), suggesting that increase in population of *cis* configuration of the methine chains enhances the intensity of the longer wavelength band. Since the heat of formation calculated with the MM2 method for the mono-*cis* and the di-*cis* conformers were only 8.0 and 11 kJ mol^{-1} larger than that of the all-*trans* conformer, respectively, the *cis*-isomers are populated to a considerable extent even at room temperature. The nearly equal strength of the two absorption bands of **1** in solution is probably due to the presence of the mono-*cis* or the di-*cis* conformer. The optimized structures of the *cis* conformer of **1** with the MM2 method indicated that the two cyanine moieties were nearly perpendicular and the splitting of the absorption bands of the *cis* conformer is mainly attributed to the orbital interactions, as in the case of the all-*trans* conformer. The splitting of the HOMO levels of the all-*trans* conformer of **1** was calculated with the INDO/S-CI method to be 0.33 eV, which corresponds to 2660 cm^{-1}. This value is nearly equal to the observed splitting (2210 cm^{-1}).

Table 3. Absorption Spectra of Mono-*cis* and Di-*cis* Conformers of **1** Calculated with the INDO/S-CI Method[a)]

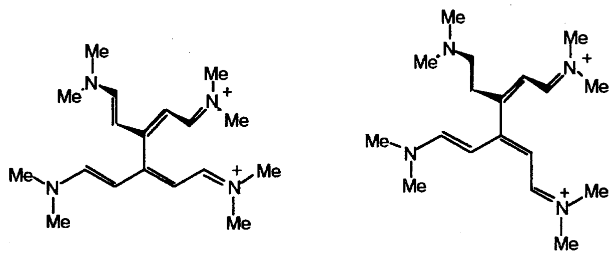

mono-*cis* di-*cis*

Compounds	λ_{max}/nm ($f^{b)}$)
Mono-*cis*	428 (0.46), 414 (0.85), 385 (0.60), 369 (0.62)
Di-*cis*	412 (0.55), 411 (0.62), 369 (0.32), 364 (0.50)

a) The MM2 optimized structures were used. b) Oscillator strengths.

Crystal Absorption Spectra. The crystal absorption spectrum of **1b** was obtained by a Kramers–Krönig transformation[12)] of a reflection spectrum from the (100) face of a single-crystal, showing a peak at 500 nm which was red-shifted compared to that of **1b** in solution. The crystal absorption is regarded as a *J*-band, a red-shifted absorption band of dye aggregates. The brickwork-like molecular stacking of **1b** in a single crystal as shown in Fig. 3 coincides with a *J*-aggregate model based upon a molecular exciton theory.[2)]

Unfortunately, the reflection spectrum in a region below 400 nm remains unmeasured because of instrumental limitations.

Fluorescence Spectra. The fluorescence spectrum of **1a** in methanol at 200 K indicated only one broad band with a peak at 600 nm and a shoulder at 660 nm (Fig. 8). The shape of a fluorescence band with the excitation at 446 nm was almost identical with that with the excitation at 406 nm, suggesting that the higher excited state (S_2) immediately changes to the lower excited state (S_1) and the fluorescence originates from the same excited state (S_1).

The fluorescence maximum of the corresponding monomer **2a** in methanol was 440 nm. The Stokes shifts for both bands of **1a** (5800 and 8100 cm^{-1} for 446 and 406 nm bands, respectively) were larger than that of **2a** (1600 cm^{-1}).

These large Stokes shifts for **1a** are probably because of the large difference in shape between the HOMO and the LUMOs for **1a**. The orbital coefficients of the HOMO are delocalized on the two cyanine moieties, while those of the LUMOs are localized on one cyanine moiety (Fig. 6).

Redox Potentials. Redox potentials for **1a** and **2a** measured with polarography are summarized in Table 4. The reduction potential for **1a** is 0.46 V positively shifted to that

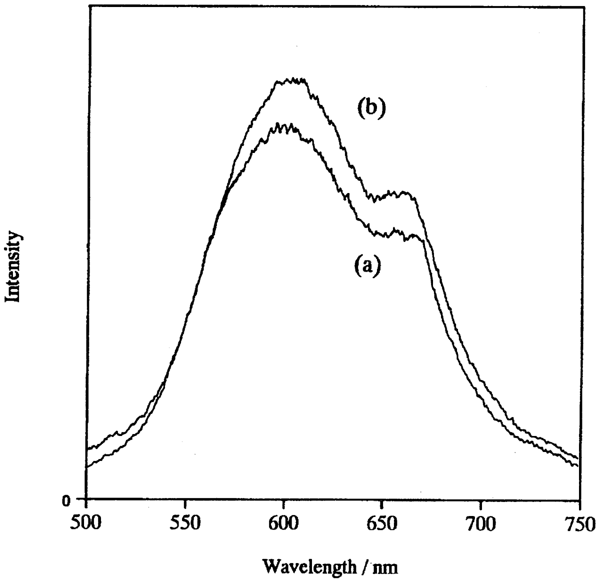

Fig. 8. Fluorescence spectra of a streptocyanine dimer **1a** in methanol at 200 K with excitation at (a) 445 nm and (b) 406 nm.

Table 4. Redox Potentials of the Streptocyanine Dimer **1a** and the Monomer **2a** Measured with Direct Current Polarography

Compounds	E_{ox} (V vs. SCE)[a)]	E_{red} (V vs. SCE)[b)]
1a	0.94, 1.18	−0.90
2a	0.98	−1.36

a) Oxidation potentials in CH_3CN containing 0.1 M $NaClO_4$.
b) Reduction potentials in CH_3CN containing 0.1 M n-Pr_4NClO_4.

for **2a**. This positive shift may be due to the Coulombic interaction between an electron and cationic charges; a cyanine dimer **1a** has two charges per one molecule, while a cyanine monomer **2a** has one charge.

The oxidation polarogram of **1a** consists of two waves due to two-stage one-electron oxidation. The lowest oxidation potential for **1a** is 0.04 V negative than that for **2a**. This negative shift can be explained by the destabilization of HOMO through spiro-conjugation, as discussed above. Similar negative shifts of the oxidation potentials were reported on biscyanine dyes **3c**.[7c)]

The two oxidation waves for **1a** are probably caused by the Coulombic interaction between an electron and cationic charges generated on the first oxidation. Similar splittings of oxidation potentials were reported on bis-tetrathiafluvalenes and explained in terms of Coulombic interactions.[13)] The magnitudes of the Coulombic interaction on bis-tetrathiafluvalenes were estimated to be 0.10—0.25 V, which is in agreement with the present observation for the cyanine dimer **1** (0.24 V).

Conclusion. Perpendicularly-linked pentamethinestreptocyanine dimers **1** were prepared. The splitting of the absorption band in solution is attributed to the splitting of HOMO levels through spiro-conjugation between the two cyanine moieties. The positive shift of the reduction potential for **1** compared to the monomer **2** is explained by the Coulombic interaction, while the negative shift of oxidation potential for **1** is due to the orbital interactions through spiro-conjugation. These results for **1** indicate that orbital–orbital interactions as well as dipole–dipole interactions play an important role in the aggregates of cyanine dyes.

Experimental

Melting points were uncorrected. ^{1}H NMR spectra were determined on a Bruker ARX-300 (300 MHz) spectrometer and chemical shifts are quoted in ppm downfield from $SiMe_4$. Infrared spectra were recorded using a JASCO IR-810 spectrometer. UV/vis spectra were recorded on a Shimadzu UV-3100PC spectrometer. FAB-Mass spectra were measured by a JEOL DX-303 mass spectrometer.

A reflection spectrum was measured on a Carl Zeiss microscopic spectrophotometer UMSP50. The reflectivities were converted to absorption coefficients by a Kramers–Krönig transformation. The computation program was based upon the method of Ahrenkiel.[13)]

The X-ray diffraction data collection was performed on a Rigaku four-circle AFC-5R diffractometer using a graphite monochromated Cu$K\alpha$ radiation and a $2\theta/\omega$ scan technique. The structure was solved by a direct method SHELXS 86.[14)] Redox potential measurements were carried out on a Yanaco polarographic analyzer P-1100. Reduction potentials were measured with a mercury working electrode and a saturated calomel electrode in CH_3CN with 0.1 M $NaClO_4$ (1 M= 1 mol dm^{-3}). Oxidation potentials were measured with a rotating Pt working electrode and a saturated calomel electrode in CH_3CN with 0.1 M n-Pr_4NClO_4. Acetonitrile for electrochemistry was dried over molecular sieves 4 Å.

All MO calculations were performed on a SONY Tektronix CAChe system. Molecular structures were optimized with a PM3 method[8)] or a MM2 method.[11)] The electronic spectra were calculated with an INDO/S-CI method[10)] considering 20 configuration interaction levels.

1,1′-Bis(2,4-dinitrophenyl)-4,4′-bipyridinium dichloride was purchased from Tokyo-Kasei Co. and (5-dimethylamino-2,4-pentadienylidene)dimethylammonium perchlorate (**2a**) was prepared by the method of Malhotra and Whiting.[15)]

Preparation of *N,N*′-[3,4-Bis[2-(dimethylamino)ethenyl]-2,4-hexadiene-1,6-diylidene]bis(dimethylammonium perchlorate) (1a). To an ethanol solution (30 ml) of 1,1′-bis(2,4-dinitrophenyl)-4,4′-bipyridinium dichloride (5.61 g, 10 mmol) was added at 0 °C 50% aqueous dimethylamine (6.0 ml), and the solution was stirred for 30 min. After water (30 ml) was added to the resulting solution, the reaction mixture was filtered. The aqueous filtrate was washed with diethyl ether (10 ml×3), and $NaClO_4 \cdot H_2O$ (3.0 g, 21 mmol) was added. The precipitate was filtered off, washed with diethyl ether, and dried to afford **1a** as yellow crystals (2.48 g, 49%); mp 195—198 °C (decomp); UV/vis (MeOH) λ_{max} (ε) 445 (60000), 404 (66500) nm; ^{1}H NMR ($CDCl_3$) δ =3.16 (s, 12H), 3.35 (s, 12H), 5.92 (d, 4H, J = 12 Hz), 7.41 (d, 4H, J = 12 Hz); IR (KBr) 2940, 1595, 1520, 1460, 1418, 1381, 1250, 1208, 1095, 875, 740, 620 cm^{-1}; MS(FAB) m/z 403 (M-ClO_4^-). Found: C, 42.86; H, 6.26; N, 10.90%. Calcd for $C_{18}H_{32}Cl_2N_4O_8$: C, 42.95; H, 6.41; N, 11.13%.

Preparation of *N,N*′-[3,4-Bis[2-(dimethylamino)ethenyl]-2,4-hexadiene-1,6-diylidene]bis(dimethylammonium hexafluorophosphate) (1b). To an ethanol solution (30 ml) of 1,1′-bis(2,4-dinitrophenyl)-4,4′-bipyridinium dichloride (5.0 g, 8.9 mmol) was added at 0 °C 50% aqueous dimethylamine (6.0 ml), and the solution was stirred for 1 h. After water (30 ml) was added to the resulting solution, the reaction mixture was filtered. The aqueous filtrate was washed with diethyl ether (10 ml×3), and $NaPF_6$ (5.0 g, 30 mmol) was added. The precipitates were filtered off, washed with diethyl ether, and dried to afford **1b** as orange crystals (2.40 g, 45%); mp 155—160 °C (decomp); UV/vis (MeOH) λ_{max} (ε) 445 (60000), 404 (66500) nm; ^{1}H NMR (CD_3OD) δ = 3.20 (s, 12H), 3.36 (s, 12H), 6.01 (d, 4H, J = 13 Hz), 7.45 (d, 4H, J = 13 Hz); IR (KBr) 2948, 2825, 1590, 1520, 1465, 1430, 1390, 1250, 1200, 1108, 958, 840, 740 cm^{-1}; FAB-MS m/z 449 (M−PF_6^-). Found: C, 36.24; H, 5.33; N, 9.26%. Calcd for $C_{18}H_{32}F_{12}N_4P_2$: C, 36.37; H, 5.43; N, 9.43%.

X-Ray Crystallographic Analysis of 1b.[16)] A single crystal of a streptocyanine dimer **1b** was obtained by recrystallization from acetone. The structure was refined by a full matrix least squares procedure to R = 0.090.

Crystal Data: Monoclinic, $P2_1/a$, a=11.689(2), b=20.558(1), c = 13.573(1) Å, β = 107.90(1)°, total unique data 4796, No. of observations [$I \geqq 5\sigma(I)$] 3069, R = 0.090, R_{w} = 0.096.

References

1) D. Möbius, *Adv. Mater.*, **7**, 437 (1995); N. Tyutyulkov, J. Fabian, A. Mehlhorn, F. Dietz, and A. Tadjer, "Polymethine Dyes," St. Kliment Ohridski University Press, Sofia (1991); A. H. Herz,

Photogr. Sci. Eng., **18**, 323 (1974); T. Tani, "Photographic Sensitivity," Oxford University Press, New York (1995), Chap. 5, pp. 111—164; W. West and P. B. Gilman, "The Theory of the Photographic Process," 4th ed, ed by T. H. James, McMillan Publ. Co., New York (1977), Chap. 10, p. 194; P. B. Gilman, *Pure Appl. Chem.*, **49**, 357 (1977); W. West, *Photogr. Sci. Eng.*, **18**, 35 (1974).

2) E. G. McRae and M. Kasha, *J. Chem. Phys.*, **28**, 721 (1958); M. Kasha, H. R. Rawis, and M. A. El-Bayoumi, *Pure Appl. Chem.*, **11**, 371 (1965); G. S. Levinson, W. T. Simpson, and W. Curtius, *J. Am. Chem. Soc.*, **79**, 4314 (1957); K. Norland, A. Ames, and T. Taylor, *Photogr. Sci. Eng.*, **14**, 295 (1970).

3) N. Berova, D. Gargiulo, F. Derguini, K. Nakanishi, and N. Harada, *J. Am. Chem. Soc.*, **115**, 4769 (1993); D. Gargiulo, F. Derguini, N. Berova, K. Nakanishi, and N. Harada, *J. Am. Chem. Soc.*, **113**, 7046 (1991).

4) K. Y. Burshtein, *Chem. Phys. Lett.*, **239**, 195 (1995); M. S. Gudipati, *J. Phys. Chem.*, **98**, 9750 (1994).

5) P. M. Kazmaier and R. Hoffmann, *J. Am. Chem. Soc.*, **116**, 9684 (1994).

6) D. L. Smith, *Photogr. Sci. Eng.*, **18**, 309 (1974).

7) a) M. Hanke and C. Jutz, *Angew. Chem., Int. Ed. Engl.*, **18**, 214 (1979); b) Z. Arnold, *Collect. Czech. Chem. Commun.*, **27**, 2993 (1962); c) R. L. Parton and J. R. Lenhard, *J. Org. Chem.*, **55**, 49 (1990).

8) J. J. P. Stewart, *J. Comput. Chem.*, **10**, 209 (1989).

9) H. E. Simmons and T. Fukunaga, *J. Am. Chem. Soc.*, **89**, 5208 (1967); R. Hoffmann, A. Imamura, and G. D. Zeiss, *J. Am. Chem. Soc.*, **89**, 5215 (1967).

10) J. Ridley and M. C. Zerner, *Theor. Chim. Acta (Berlin)*, **32**, 111 (1973).

11) N. L. Allinger, *J. Am. Chem. Soc.*, **99**, 8127 (1977).

12) R. K. Ahrenkiel, *J. Opt. Soc. Am.*, **61**, 165 (1971).

13) M. Adam and K. Müllen, *Adv. Mater.*, **6**, 439 (1994); T. Otsubo, Y. Aso, and K. Takimiya, *Adv. Mater.*, **8**, 203 (1996).

14) G. M. Sheldrick, "Crystallographic Computing 3," ed by G. M. Sheldrick, C. Kruger, and R. Goddard, Oxford University Press, Oxford (1985), p. 175.

15) S. S. Malhotra and M. C. Whiting, *J. Chem. Soc.*, **1960**, 3812.

16) Full crystal data, atom coordinates, thermal parameters, and bond distances and angles are deposited as Document No. 70012 at the Office of the Editor of Bull. Chem. Soc. Jpn.